

1

2 **Supplementary Information for**

3 **Sea-surface temperature pattern effects have slowed global warming and biased** 4 **warming-based constraints on climate sensitivity**

5 **Kyle C. Armour, Cristian Proistosescu, Yue Dong, Lily C. Hahn, Edward Blanchard-Wrigglesworth, Andrew G. Pauling, Robert**
6 **C. Jnglin Wills, Timothy Andrews, Malte F. Stuecker, Stephen Po-Chedley, Ivan Mitevski, Piers M. Forster, and Jonathan M.**
7 **Gregory**

8 **Kyle Armour**
9 **E-mail: karmour@uw.edu**

10 **This PDF file includes:**

11 Supplementary text
12 Figs. S1 to S7
13 Tables S1 to S2

14 **Supporting Information Text**

15 **Tables S1 and S2**

16 Tables S1 and S2 show relevant parameters for CMIP5 and CMIP6 models, respectively. This includes the number of *historical*
17 ensemble members used in the analysis in the main text; equilibrium climate sensitivity (ECS); transient climate response
18 (TCR); and two-layer energy balance model (EBM) parameter values. Also noted are which models are included in our
19 eight-model subset.

20 **The relationship between post-1970s warming rate and transient climate response**

21 Fig. S1 shows the equivalent of Fig. 1 in the main text, but for the relationship between TCR and the 1981-2014 warming rate
22 or effective climate sensitivity (EffCS). TCR values are calculated from the global temperature change near year 70 (time of
23 CO₂ doubling) of CMIP5/6 1%/yr CO₂ ramping simulations (*1pctCO2*). See Fig. S4 for the relationships between TCR and
24 the 1981-2014 warming rate when accounting for observed sea-surface temperature (SST) trend patterns.

25 **The relationship between SST trend patterns, EffCS, and global warming rate in the CESM1-CAM5 large ensemble**

26 Fig. S2 shows regressions between local SST trend patterns and either global warming rates or EffCS over 1981-2014. Also
27 shown is the relationship between EffCS and warming rate over 1981-2014 when using the CAM5 Green's function of Zhou et
28 al. (22) combined with SST trend patterns to estimate radiative feedback and EffCS (Fig. S2c), rather than regression methods
29 as in Fig. 1d of the main text.

30 **Correcting for warming rates using model-specific relationships between EffCS and warming rates over 1981-2014**

31
32 Figs. S3 and S4c,d show the equivalent of Figs. 1d and 3a in the main text, but using model-specific relationships between
33 EffCS and warming rates over 1981-2014 in the estimate of the warming rate in each model had it simulated the observed SST
34 trend pattern.

35 **Two-layer energy balance model (EBM) simulations**

36 Figure S5 shows the equivalent of Fig. 1 in the main text, but for the EBM response to historical (to 2014) and RCP8.5 (to
37 2100) ERF as described in the Methods. Figure S7a shows the EBM response to historical and RCP8.5 ERF over 1850-2100
38 using parameters fit to CMIP5/6 models (see Methods, and Tables S1-2). We also run the EBM under a linear increase in ERF
39 representing 1%/yr CO₂ ramping simulations (to calculate EBM values of TCR, as in the CMIP5/6 models).

40 Figure S6a shows EffCS within the EBM, illustrating that EffCS values are near ECS values for each ensemble member.
41 EffCS is calculated from the linear regression of global radiative response and global surface warming (Methods) within
42 running 34-year windows (the length of the period 1981-2014), and EffCS values vary over time depending on the degree of
43 disequilibrium between the upper and lower ocean layers owing to the efficacy of ocean heat uptake parameter (Methods). To
44 illustrate the impact of changing EffCS on projected warming, we introduce a linear trend in the radiative feedback λ such that
45 EffCS $\approx 2^\circ\text{C}$ over the period 1981-2014 for each CMIP5/6 parameter set (Fig. S6b), with this value of EffCS chosen to match
46 observed energy budget constraints and *amip* simulations (see main text). This produces the 1981-2014 warming rates shown
47 by the diamonds in Fig. S5 and Fig. 3c.

48 We also perform several extensions of these simulations with various hypothetical evolutions of λ and EffCS over the period
49 2015-2100. We consider three scenarios: (i) λ remains constant over the period 2015-2100, thus maintaining EffCS $\approx 2^\circ\text{C}$
50 (Fig. S6b); (ii) λ is linearly returned to CMIP5/6 model values by 2050 (reversing the linear λ trend applied over 1981-2014
51 in approximately the same number of years) (Fig. S6c); and (iii) λ is linearly returned to CMIP5/6 model values by 2100
52 (reversing the linear λ trend applied over 1981-2014 but more slowly) (Fig. S6d). Figure S7 shows the EBM temperature
53 response in each of these scenarios.

Table S1. CMIP5 model ECS, TCR, and two-layer energy balance model (EBM) parameter values. Number of *historical* ensemble members used in the analysis listed in parentheses. Models included in the eight-model subset in the main text denoted by *.

Model	Two-layer EBM parameters fit to <i>abrupt4xCO2</i> simulations							
	ECS (K)	TCR (K)	C ($\text{W yr m}^{-2}\text{K}^{-1}$)	C_0 ($\text{W yr m}^{-2}\text{K}^{-1}$)	λ ($\text{Wm}^{-2}\text{K}^{-1}$)	γ ($\text{Wm}^{-2}\text{K}^{-1}$)	ε	$\text{ERF}_{2\times}$ (Wm^{-2})
ACCESS1-0 (1)	3.90	1.77	8.9	83	-0.81	0.71	1.55	3.6
ACCESS1-3 (1)	3.63	1.60	10.1	114	-0.81	0.72	1.62	3.5
bcc-csm1-1 (1)	2.91	1.76	8.8	57	-1.28	0.58	1.27	3.6
CCSM4 (6)	2.94	1.80	7.8	72	-1.40	0.81	1.36	4.2
CESM1-CAM5* (40)	3.32	2.07	8.7	144	-1.22	0.60	1.19	4.3
CNRM-CM5 (1)	3.28	1.97	8.7	96	-1.12	0.51	0.92	3.5
CSIRO-Mk3-6-0 (10)	4.36	1.69	9.3	77	-0.66	0.71	1.80	3.4
CanESM2 (5)	3.71	2.30	8.3	77	-1.05	0.54	1.28	4.1
GFDL-CM3 (3)	4.03	1.76	9.9	76	-0.78	0.71	1.39	3.4
GFDL-ESM2G (1)	2.34	1.21	6.5	104	-1.48	0.80	1.17	3.5
GFDL-ESM2M (1)	2.46	1.37	8.9	113	-1.38	0.86	1.23	3.6
GISS-E2-H (5)	2.43	1.78	10.5	86	-1.64	0.70	1.27	4.1
GISS-E2-R (6)	2.28	1.48	6.1	135	-2.03	1.07	1.44	4.6
HadGEM2-ES (4)	4.64	2.43	8.3	99	-0.60	0.49	1.57	3.4
inmcm4 (1)	2.05	1.29	9.1	277	-1.57	0.69	1.82	3.0
IPSL-CM5A-LR (4)	4.05	1.97	8.6	100	-0.79	0.57	1.14	3.3
IPSL-CM5B-LR (1)	2.64	1.44	9.7	68	-1.07	0.63	1.43	3.0
MIROC5 (5)	2.70	1.47	9.7	163	-1.58	0.74	1.20	4.4
MPI-ESM-LR (3)	3.66	2.01	9.2	78	-1.20	0.62	1.43	4.7
MRI-CGCM3 (1)	2.61	1.52	10.1	70	-1.30	0.60	1.25	3.5
NorESM1-M (1)	2.93	1.39	9.9	122	-1.15	0.76	1.57	3.6

Table S2. CMIP6 model ECS, TCR, and two-layer energy balance model (EBM) parameter values. Number of *historical* ensemble members used in the analysis listed in parentheses. Models included in the eight-model subset in the main text denoted by *.

Model			Two-layer EBM parameters fit to <i>abrupt4xCO2</i> simulations					
	ECS (K)	TCR (K)	C (W yr m ⁻² K ⁻¹)	C_0 (W yr m ⁻² K ⁻¹)	λ (Wm ⁻² K ⁻¹)	γ (Wm ⁻² K ⁻¹)	ϵ	ERF _{2x} (Wm ⁻²)
ACCESS-CM2 (3)	4.72	2.10	9.0	93	-0.71	0.53	1.55	4.0
ACCESS-ESM1-5 (20)	3.87	1.95	9.0	97	-0.72	0.60	1.73	3.5
AWI-CM-1-1-MR (5)	3.16	2.06	8.3	57	-1.22	0.46	1.49	4.1
BCC-CSM2-MR (3)	3.02	1.72	6.5	64	-1.20	0.84	1.37	3.8
BCC-ESM1 (3)	3.26	1.77	8.9	98	-0.91	0.52	1.39	3.3
CAMS-CSM1-0 (7)	2.29	1.73	10.2	61	-1.87	0.47	1.29	4.4
CanESM5* (25)	5.64	2.74	8.0	80	-0.65	0.52	1.07	3.8
CESM2 (11)	5.15	2.06	8.7	75	-0.69	0.66	1.89	4.5
CESM2-WACCM (3)	4.68	1.98	8.5	89	-0.74	0.69	1.57	4.1
CMCC-CM2-SR5 (1)	3.52	2.09	8.9	79	-1.06	0.41	1.27	4.0
CNRM-CM6-1* (30)	4.90	2.14	7.6	147	-0.74	0.50	1.00	3.6
CNRM-CM6-1-HR (1)	4.33	2.48	8.2	95	-0.92	0.55	0.72	3.7
CNRM-ESM2-1 (10)	4.79	1.86	7.5	100	-0.63	0.59	0.91	2.9
E3SM-1-0 (3)	5.31	2.99	8.6	44	-0.63	0.35	1.50	3.7
EC-Earth3 (73)	4.10	2.30	8.1	37	-0.81	0.42	1.42	3.7
EC-Earth3-Veg (8)	4.33	2.62	8.4	40	-0.82	0.40	1.42	3.8
FGOALS-f3-L (3)	2.98	1.94	9.3	88	-1.41	0.53	1.58	4.7
FGOALS-g3 (5)	2.88	1.54	7.8	98	-1.30	0.69	1.30	4.0
GISS-E2-1-G* (12)	2.71	1.80	6.7	144	-1.47	0.84	1.10	4.1
GISS-E2-1-H (25)	3.12	1.93	8.9	86	-1.15	0.61	1.20	3.7
HadGEM3-GC31-LL* (5)	5.55	2.55	8.0	77	-0.63	0.51	1.22	3.7
HadGEM3-GC31-MM (4)	5.42	2.58	8.3	73	-0.66	0.58	1.03	3.6
INM-CM4-8 (1)	1.83	1.33	6.4	26	-1.68	0.78	1.31	3.1
IPSL-CM6A-LR* (32)	4.56	2.32	8.2	63	-0.75	0.41	1.33	3.7
KACE-1-0-G (3)	4.48	1.41	9.0	120	-0.71	0.74	1.31	3.8
MIROC-ES2L (11)	2.66	1.55	10.6	185	-1.56	0.67	0.93	4.1
MIROC6* (50)	2.60	1.55	8.9	175	-1.38	0.65	1.32	3.9
MPI-ESM-1-2-HAM (3)	2.96	1.80	9.5	113	-1.44	0.64	1.34	4.5
MPI-ESM1-2-HR (8)	2.98	1.66	8.9	84	-1.33	0.66	1.50	4.3
MPI-ESM1-2-LR (10)	3.00	1.84	9.5	114	-1.40	0.59	1.23	4.4
MRI-ESM2-0 (6)	3.13	1.64	8.7	96	-1.21	0.85	1.43	4.1
NESM3 (5)	4.77	2.72	5.6	105	-0.78	0.46	0.97	3.7
NorCPM1 (29)	3.05	1.56	9.9	108	-1.18	0.78	1.55	4.0
NorESM2-LM* (3)	2.56	1.48	5.6	119	-1.71	0.86	1.99	5.0
NorESM2-MM (3)	2.50	1.33	6.0	114	-1.74	0.79	1.66	4.8
SAM0-UNICON (1)	3.72	2.27	7.3	100	-1.09	0.79	1.24	4.3
TaiESM1 (1)	4.31	2.34	8.8	97	-0.93	0.63	1.34	4.4
UKESM1-0-LL (18)	5.36	2.79	8.0	80	-0.67	0.52	1.12	3.7

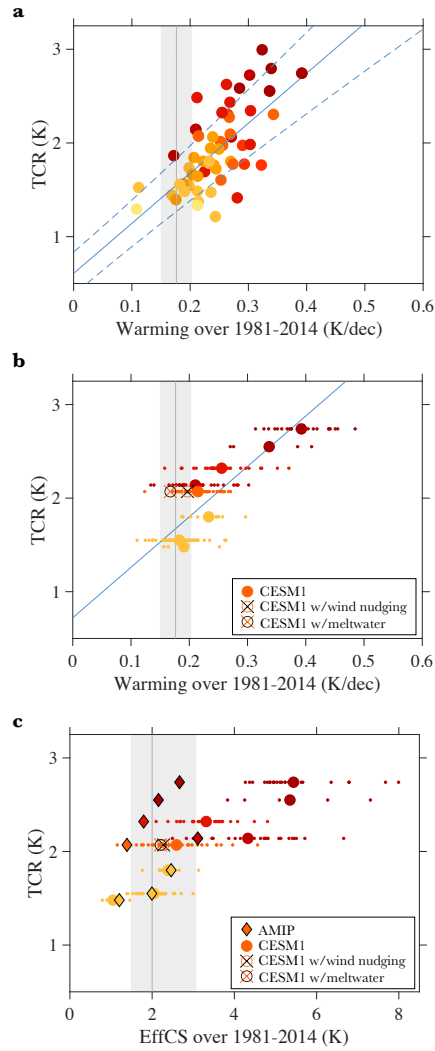


Fig. S1. Relationships between transient climate response (TCR), effective climate sensitivity (EffCS), and the 1981-2014 warming rate in CMIP5/6 models. a, CMIP5/6 TCR versus warming rate using averages of all available ensemble members for each model ($r^2 = 0.46$); colors correspond to values of ECS. **b,** Eight-model subset TCR versus warming rate with ensemble means shown as larger circles and ensemble members shown as smaller dots. **c,** Eight-model subset TCR versus EffCS over 1981-2014 with ensemble means shown as larger circles and ensemble members shown as smaller dots; diamonds show EffCS values from AGCM simulations forced by observed SST trend patterns. In **b,c**, open circles show CESM1-CAM5 simulations with wind nudging or meltwater forcing as described in the main text. Blue lines show fits calculated using ordinary least squares regression, with dashed blue lines showing 5-95% ranges of fit parameters. Gray shading shows observational estimates (5-95% range) of observed warming rate and EffCS as described in the main text.

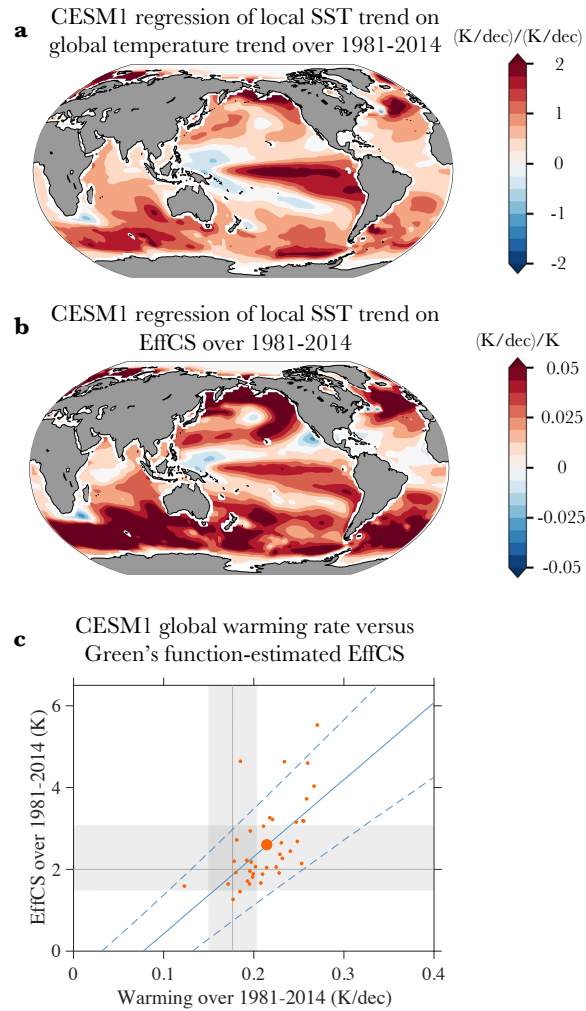


Fig. S2. The relationship between SST trend patterns, EffCS, and 1981-2014 warming rate in the CESM1 large ensemble. **a**, Regression between local SST trends and global warming rates across ensemble members. **b**, Regression between local SST trends and EffCS values (calculated as described in main text) across ensemble members. **c**, Green's function-estimated EffCS (calculated using the CAM5 Green's function of Zhou et al. (22) convolved with SST trend pattern of each ensemble member) versus warming rate over 1981-2014, with ensemble mean shown as larger circles and ensemble members shown as smaller dots ($r^2 = 0.36$). Blue lines show fit calculated using ordinary least squares regression, with dashed blue lines showing 5-95% ranges of fit parameters. Gray shading shows observational estimates (5-95% range) of observed warming rate and EffCS as described in the main text.

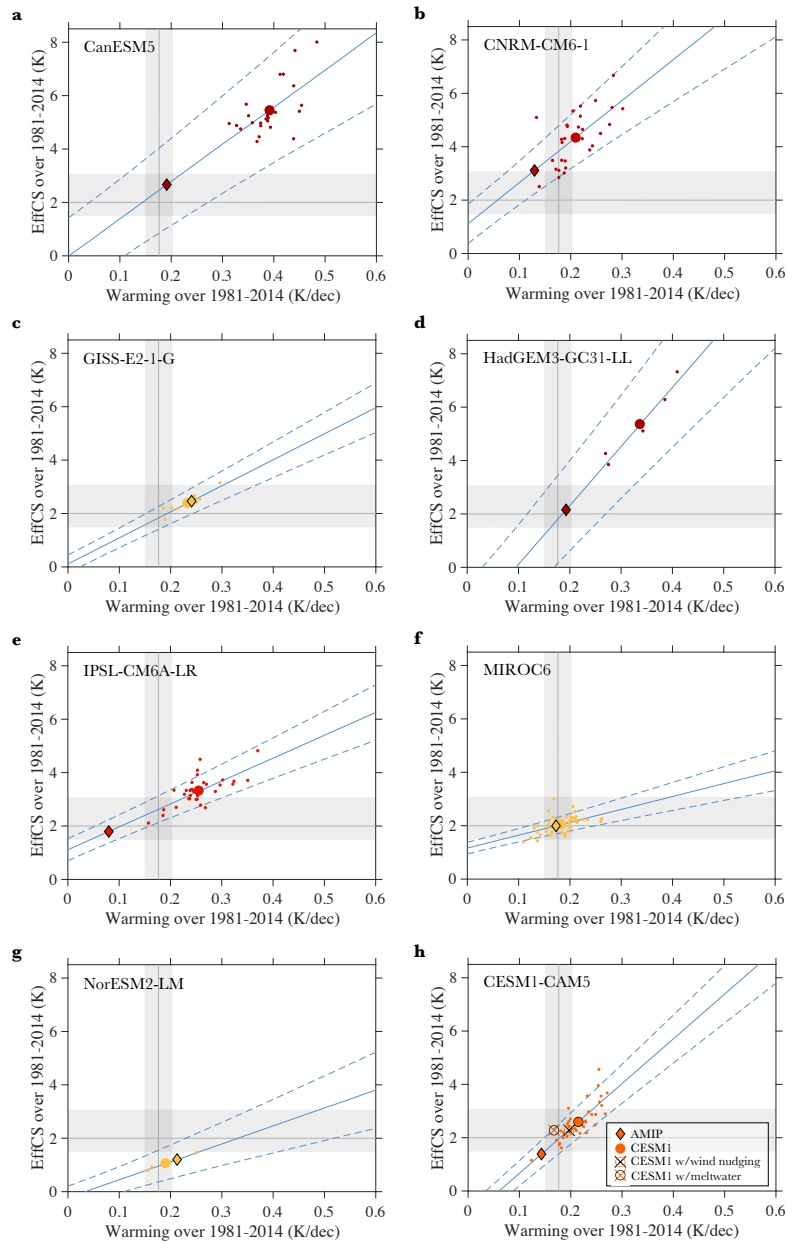


Fig. S3. Relationships between effective climate sensitivity (EffCS) over 1981-2014 and 1981-2014 warming rate in individual CMIP5/6 models. a, CanESM5. b, CNRM-CM6-1. c, GISS-E2-1-G. d, HadGEM3-GC31-LL. e, IPSL-CM6A-LR. f, MIROC6. g, NorESM2-LM. h, CESM1-CAM5. Ensemble means shown as larger circles and ensemble members shown as smaller dots. Also shown are EffCS and warming rates in CESM1-CAM5 simulations with wind nudging or meltwater forcing (see main text). Blue lines show fits calculated using ordinary least squares regression, with dashed blue lines showing 5-95% ranges of fit parameters. Gray shading shows observational estimates (5-95% range) of observed warming rate (HadCRUT5) and EffCS (see main text). Diamonds show EffCS values from AGCM simulations forced by observed warming patterns, with the corresponding warming rates estimated from the regression between EffCS over 1981-2014 and warming rate for each model (blue line).

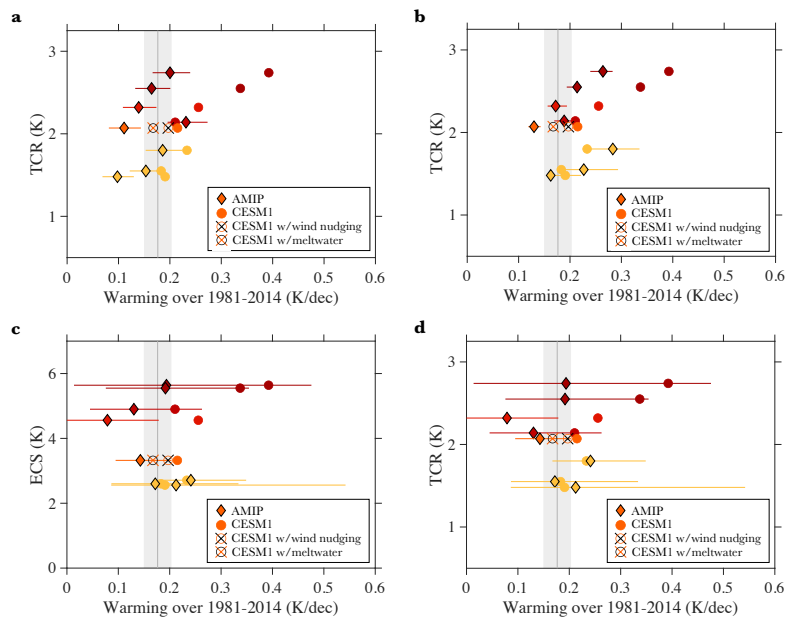


Fig. S4. Relationships between climate sensitivity metrics and the 1981-2014 warming rate with (diamonds) and without (circles) accounting for observed warming patterns. TCR vs warming rate for **a**, CMIP5/6 eight-model subset, with circles showing uncorrected warming rates (from Fig. 1b) and diamonds showing corrected warming rates estimated using AGCM values of EffCS and the relationship between EffCS and warming (Fig. 1d); horizontal lines show 5-95% confidence ranges from uncertainty in the fit. **b**, CMIP5/6 eight-model subset, with circles showing uncorrected warming rates (Fig. S1b) and diamonds showing corrected warming rates estimated using AGCM values of λ and equation (3), with horizontal lines showing uncertainty ranges reflecting the spread in κ across ensemble members. **c**, CMIP5/6 ECS vs warming rate, with corrected warming rates (diamonds) estimated using AGCM values of EffCS and the relationship between EffCS and warming in the individual CMIP5/6 models (Fig. S3), with horizontal lines showing 5-95% confidence ranges from uncertainty in the fit; circles show uncorrected values as in Fig. 1b. **d**, CMIP5/6 TCR vs warming rate, with corrected warming rates (diamonds) estimated using AGCM values of EffCS and the relationship between EffCS and warming in the individual CMIP5/6 models (Fig. S2), with horizontal lines showing 5-95% confidence ranges from uncertainty in the fit; circles show uncorrected values as in Fig. S1b. Gray shading shows observational estimates (5-95% range) of observed warming rate as described in the main text.

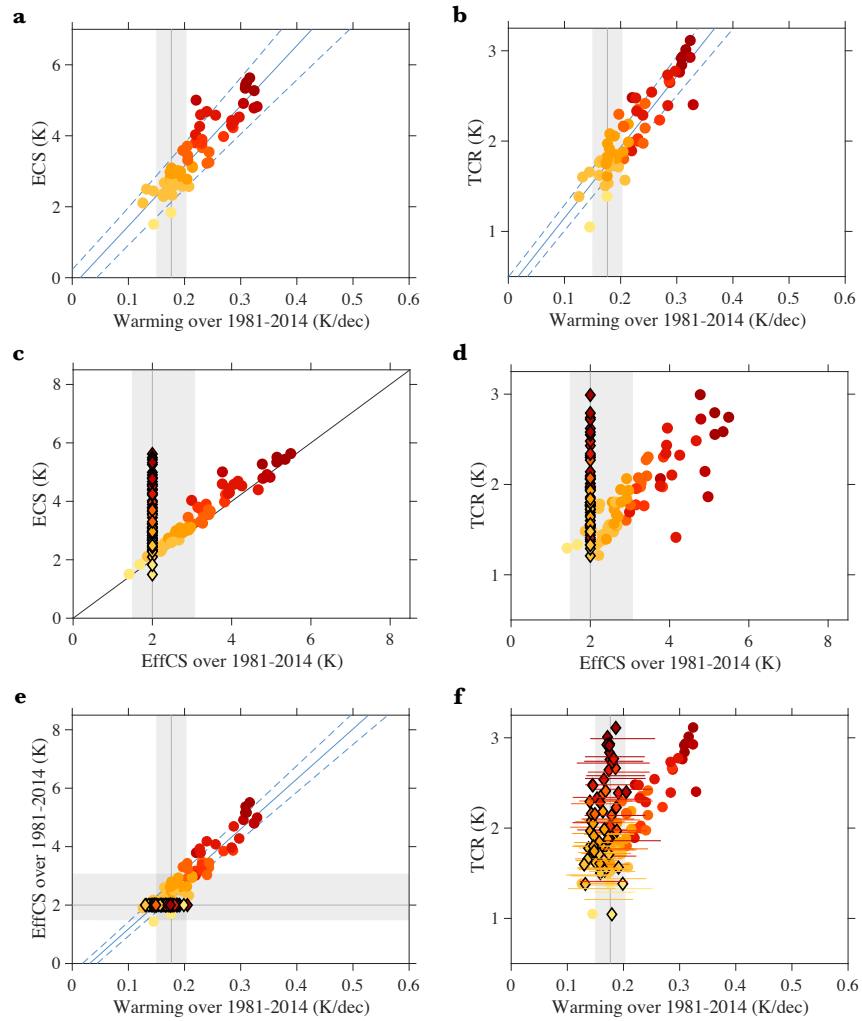


Fig. S5. Relationships between equilibrium climate sensitivity (ECS), transient climate response (TCR), effective climate sensitivity (EffCS), and the 1981-2014 warming rate in the two-layer energy balance model (EBM). **a**, ECS versus warming rate; colors correspond to values of ECS. **b**, TCR versus warming rate. **c**, ECS versus EffCS over 1981-2014; diamonds show an EffCS value corresponding to an observational estimate of 2°C. **d**, TCR versus EffCS over 1981-2014; diamonds show an EffCS value corresponding to an observational estimate of 2°C. **e**, EffCS over 1981-2014 versus warming rate; diamonds show warming rates simulated by the EBM when using an EffCS value corresponding to an observational estimate of 2°C over 1981-2014, which are in good agreement with the regression slope (blue line with dashed blue lines showing 5-95% ranges of fit parameters). **f**, Relationship between TCR and warming rate with circles showing uncorrected warming rates and diamonds showing corrected warming rates using observed values of EffCS as described in main text, with a median of 2°C and horizontal lines showing 5-95% confidence ranges showing 1.5-3.1°C. Gray shading shows observational estimates (5-95% range) of observed warming rate and EffCS as described in the main text.

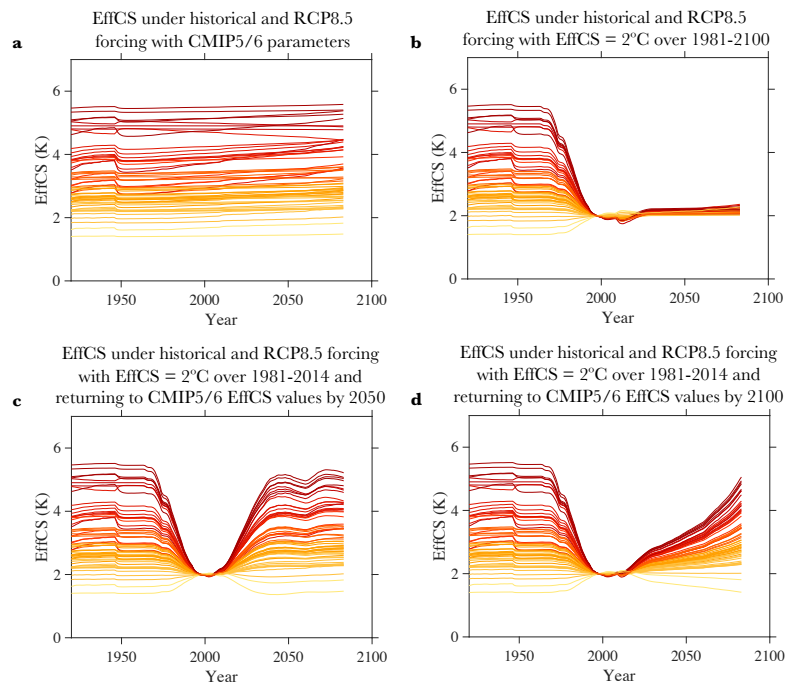


Fig. S6. Two-layer energy balance model (EBM) effective climate sensitivity (EffCS) under historical and RCP8.5 radiative forcing, either with CMIP5/6 model parameters or with prescribed changes in EffCS. a, EffCS using CMIP5/6 parameters; colors correspond to values of ECS. **b,** EffCS using CMIP5/6 parameters but with EffCS = 2°C over 1981-2100. **c,** EffCS using CMIP5/6 parameters but with EffCS = 2°C over 1981-2014 and EffCS returning to CMIP5/6 values by 2050. **d,** EffCS using CMIP5/6 parameters but with EffCS = 2°C over 1981-2014 and EffCS returning to CMIP5/6 values by 2100.

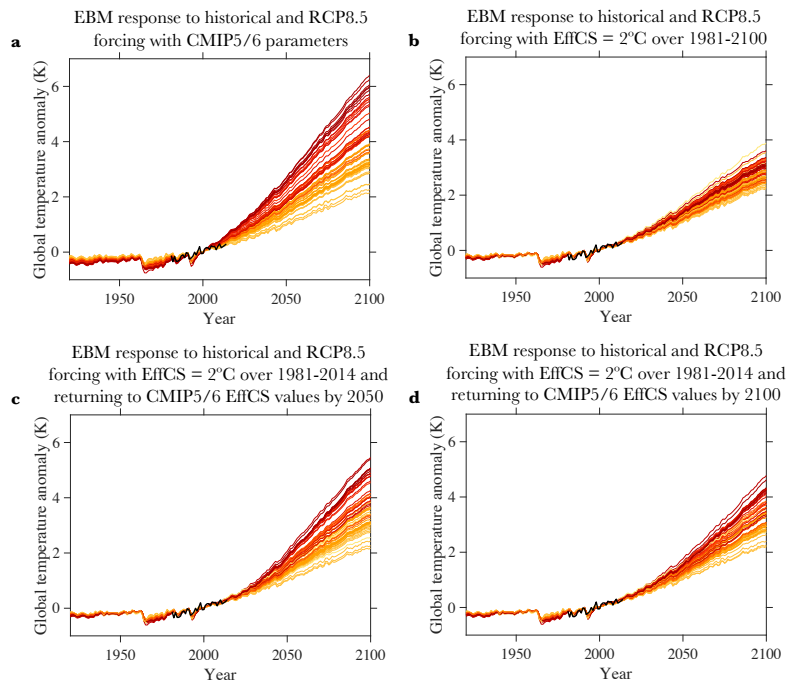


Fig. S7. Two-layer energy balance model (EBM) global surface temperature response to historical and RCP8.5 radiative forcing, either with CMIP5/6 model parameters or with prescribed changes in effective climate sensitivity (EffCS). **a**, Temperature anomaly using CMIP5/6 parameters; colors correspond to values of ECS. **b**, Temperature anomaly using CMIP5/6 parameters but with EffCS = 2°C over 1981-2100. **c**, Temperature anomaly using CMIP5/6 parameters but with EffCS = 2°C over 1981-2014 and EffCS returning to CMIP5/6 values by 2050. **d**, Temperature anomaly using CMIP5/6 parameters but with EffCS = 2°C over 1981-2014 and EffCS returning to CMIP5/6 values by 2100. Black lines show observed global surface temperature anomaly from HadCRUT5 over 1981-2014, and all anomalies are plotted with respect to the average over 1981-2014.